# The Use of Glass Substrates with Bi-Functional Silanes for Designing Micropatterned Cell-Secreted Cytokine Immunoassays

**Jeong Hyun Seo**[1], **Li-Jung Chen**[2], **Stanislav V. Verkhoturov**[2], **Emile A. Schweikert**[2], and **Alexander Revzin**[1,*]

[1]Department of Biomedical Engineering, University of California, Davis, CA 95616, United states

[2]Department of Chemistry, Texas A&M University, College Station, Texas 77843

## Abstract

It is often desirable to sequester cells in specific locations on the surface and to integrate sensing elements next to the cells. In the present study, surfaces were fabricated so as to position cytokine sensing domains inside non-fouling poly(ethylene glycol) (PEG) hydrogel microwells. Our aim was to increase sensitivity of micropatterned cytokine immunoassays through covalent attachment of biorecognition molecules. To achieve this, glass substrates were functionalized with a binary mixture of acrylate- and thiol-terminated methoxysilanes. During subsequent hydrogel photopatterning step acrylate moieties served to anchor hydrogel microwells to glass substrates. Importantly, glass attachment sites within the microwells contained thiol groups that could be activated with a hetero-bifunctional cross-linker for covalent immobilization of proteins. After incubation with fluorescently-labeled avidin, microwells fabricated on a mixed acryl/thiol silane layer emitted ~6 times more fluorescence compared to microwells fabricated on an acryl silane alone. This result highlighted the advantages of covalent attachment of avidin inside the microwells. To create cytokine immunoassays, micropatterned surfaces were incubated with biotinylated IFN-γ or TNF-α antibodies (Abs). Micropatterned immunoassays prepared in this manner were sensitive down to 1 ng/ml or 60 pM IFN-γ. To further prove utility of this bionterface design, macrophages were seeded into 30 µm diameter microwells fabricated on either bi-functional (acryl/thiol) or monofunctional silane layers. Both types of microwells were coated with avidin and biotin-anti-TNF-α prior to cell seeding. Short mitogenic activation followed by immunostaining for TNF-α revealed that microwells created on bi-functional silane layer had 3 times higher signal due to macrophage-secreted TNF-α compared to microwells fabricated on mono-functional silane. The rational design of cytokine-sensing surfaces described here will be leveraged in the future for rapid detection of multiple cytokines secreted by individual immune cells.

## Keywords

cell function; cytokine release and immune cells; cytokine detection; immunoassay; cell micropatterning; hydrogel microwells

*Corresponding author: Alexander Revzin, Ph.D., Department of Biomedical Engineering, UC Davis, Phone: 1-530-752-2383, arevzin@ucdavis.edu.

## INTRODUCTION

Cytokines are proteins secreted by mammalian cells in the process of endocrine communication. These proteins may be released in response to injury, causing inflammation or cell death,[1, 2] or on the contrary, protecting against tissue injury.[3] Cytokine production in leukocytes is an important means of monitoring immune competency or disease progression in patients. For example, detection of inflammatory cytokines such as IFN-γ is used for diagnosing latent form of tuberculosis.[4] In an attempt to get more detailed and nuanced understanding of the roles played by leukocyte subsets in the immune response, immunologists are becoming increasingly interested in connecting cytokine secretion profiles to specific leukocyte subsets and to specific single cells.[5–9] This goal is complicated by the fact that certain cytokines like TNF-α and IFN-γ may be secreted by multiple leukocyte subsets. Therefore, standard immunoassays of blood serum are insufficient to discern which leukocyte subsets secreted cytokines in question.

The main immunology tools used for cytokine profiling are flow cytometry and enzyme-linked immunospot (ELISpot) assays.[10–12] These technologies are robust and have been adapted by the immunology community; however, there is a need to develop new tools that are less expensive and more suited for detecting cytokine release from live cells. Microfabrication and micropatterning approaches are particularly well-suited for tackling the challenge of connecting specific cells with specific secreted signals.[13, 14] Several groups have been developing microdevices,[15–18] micropatterned surfaces[19–21] and microarrays[22–25] for leukocyte analysis. Previously, our group described the use of microarrays for capturing groups of T-cells on anti-CD4 or anti-CD8 T-cells spots (150 cells per spot) and detecting secreted cytokines on adjacent anti-cytokine antibody spots.[25] More recently, we demonstrated patterning hydrogel microwells on top of a mixed layer of anti-cell/anti-cytokine Abs to enable capturing individual CD4 T-cells from human blood and detecting IFN-γ secreted by single cells.[21] However, in these past studies Ab molecules were immobilized by physical adsorption on the glass attachment sites inside the microwells. We therefore hypothesized that orienting Ab molecules inside the microwell will improve sensitivity of micropatterned cytokine-sensing surfaces.

Surfaces functionalized with $NH_2$, SH, COOH, NHS ester or epoxide end groups are commonly used for covalent immobilization of proteins. Avidin-biotin and protein A-Ab interactions provide additional routes for oriented attachment of Ab molecules.[26] Because we are interested in using micropatterned surfaces for capturing single cells and detecting cytokines or other proteins released by the cells, our desired surface needed to have a periodic pattern of non-fouling regions and cell/cytokine adhesive domains. Micropatterning strategies described in the literature include microcontact printing, photoresist lithography and direct write/spot approaches.[27–30] Another strategy, used extensively in our previous studies, is poly(ethylene glycol) (PEG) photolithography whereby PEG prepolymer is photopatterned to create hydrogel microwells that are used to confine attachment of cells or proteins to certain regions of the glass substrate surface.[31, 32] This is a simple micropatterning strategy and can be used to populate large surface area with microwells for cell analysis.[20, 32] Attachment of hydrogel microstructures to glass or other oxide containing surfaces is typically promoted using an acrylated silane coupling agent.[20, 32]

Moving beyond simple mono-functional silane layers, we wanted to design a coupling layer that would not only anchor hydrogel microstuructures but could also be used for oriented attachment of cytokine-specific Ab molecules. Several strategies for creating multi-functional silane layers have been proposed. For example, Stenger and Dulcey developed an approach of laser desorption/patterning of silane molecules and backfilling with another

silane type to create periodic bi-functional silane surfaces.[33] We favored a simpler approach of defining composition of functional groups on the surface by random co-assembly of two different silanes.[34–36] This method was recently employed by Lee et al. to modify glass substrates with a silane layer comprised of ally- and amine-terminated silanes for covalent attachment of both hydrogel structures and avidin molecules.[37] In this paper, co-assembly of acrylate- and thiol-terminated silanes was used to create a bi-functional layer suitable for anchoring hydrogel microstructures and for oriented attachment of antibodies. These micropatterned surfaces were employed in construction of immunoassays for detection of exogenous and endogenous (cell-secreted) cytokines.

## MATERIALS AND METHODS

### Materials

Glass slides ($75 \times 25$ mm$^2$) were obtained from VWR (West Chester, PA). (3-acryloxypropyl) trimethoxysilane (MW 234) and 3-mercaptopropyl trimethoxysilane (MW 196) were purchased from Gelest, Inc. (Morisville, PA). Poly(ethylene glycol)diacrylate (PEG-DA, MW575), 2-hydroxy-2-methylpropiophenone (photoinitiator), bovine serum albumin (BSA), dimethylsulfoxide (DMSO), and anhydrous toluene (99.9%) were purchased from Sigma-Aldrich (Saint Louis, MO). MAL-PEG2-NHS ester was purchased from Quanta Biodesign, Ltd. (Powell, OH). Alexa Fluor-546 conjugated streptavidin, Alexa Fluor-488 conjugated neutravidin, and regular neutravidin were purchased from Invitrogen (Carlsbad, CA). Recombinant human IFN-γ and biotinylated goat antihuman IFN-γ Ab were purchased from R&D systems (Minneapolis, MN). Poly(dimethylsioxane) (PDMS) along with a curing agent were purchased from Dow Corning (Midland, MI).

### Silane modification of glass substrates

Prior to silanization, glass slides were cleaned by immersion in piranha solution consisting of 3 parts of 95% (v/v) sulfuric acid and 1 part of 35% (w/v) hydrogen peroxide for 10 min. Subsequently, glass slides were thoroughly rinsed with deionized (DI) water, dried under nitrogen and stored in class 10000 cleanroom. Immediately prior to silanization, glass substrates were treated in an oxygen plasma chamber (YES-R3, San Jose, CA) at 300 W for 5 min. Then the substrates were immersed for 12 h in a binary mixture of (3-acryloxypropyl) trimethoxysilane and 3-mercaptopropyl trimethoxysilane diluted to 0.1% v/v in anhydrous toluene. 1:1 molar ratio of the two silanes was used. Silanization was conducted in a glove bag filled with nitrogen to minimize atmospheric moisture. After incubation, slides were rinsed with fresh toluene, dried under nitrogen and baked at 100°C for 1 h. The silane-modified glass slides were stored in a desiccator before further use.

### Characterizing bi-functional silane layer by TOF-SIMS and AFM

Secondary ion mass spectrometry (SIMS) equipped with time of flight (ToF) spectrometer was used to examine surfaces at different steps in the modification procedure. A custom-built ToF-SIMS using primary $C_{60}^+$ of 26 keV total impact energy generates negative secondary ion emissions from the topmost layers of a negatively biased target. A feature technique is to run the ToF-SIMS in the event-by event bombardment/detection mode.[38] It has been previously determined that the secondary ions are emitted from a hemispheric volume of ~5–10nm in diameter under a single projectile impact.[39] Each single impact was detected and recorded as an individual event by a micro-channel plate (MCP) detector assembled with eight metal anodes. An accumulation of several million events comprised a conventional secondary ion mass spectrum. The event-by-event bombardment/detection approach allows us to unfold the co-emitted multiple secondary ions and extract a coincidental ion mass spectrum of co-located molecules within a nanometric impact/emission volume.[40]

Immobilization of avidin inside the microwells was also characterized topographically using AFM (MFP-3D, Asylum Research Corp.) operated in tapping mode at a scan rate of 0.5 Hz.

### Fabrication of hydrogel microwells

Photolithographic patterning of PEG hydrogel was conducted as previously described.[32] Briefly, a prepolymer solution containing PEG-DA and photoinitiator was spin-coated onto silanized substrates using Spintech S-100 (Redding, CA) operated at 800 rpm for 4 s. This prepolymer solution was then exposed to UV light (60 mWcm$^{-2}$) through a chrome/sodalime photomask for 0.5 s using UV OmniCure series 1000 light source (EXPO, Mississauga, Ontario, Canada). PEG-DA surface exposed to UV became cross-linked while unexposed PEG regions were easily dissolved in DI water. This process resulted in formation of 30 µm diameter microwells with PEG hydrogel walls and glass bottom.

### Attachment of Ab molecules on micropatterned surfaces

Micropatterned surfaces fabricated on acrylate/thiol silane layer were incubated for 2 h in 500 mM MAL-PEG2-NHS dissolved 1:1 mixture of DMSO and 1× PBS (see Figure 1B). To analyze immobilization of avidin, microwells created on mono-functional (acrylated silane only) and bi-functional silane layers were incubated with streptavidin-Alexa 546 and imaged using Agilent microarray scanner. GenePix Pro 6.0 software (Molecular Devices, Downingtown, PA) was used for quantification of fluorescent intensity. For cytokine capture and detection experiments, microwell arrays were incubated in 1mg/mL of neutravidin for 1 h, followed by incubation with 5 µg/mL of biotinylated IFN-γ or TNF-α Ab. These surfaces were then challenged with recombinant IFN-γ of varying concentrations (from 1 ng/ml to 10 µg/ml). The presence of cytokine molecules on micropatterned surfaces was determined by attaching biotinylated anti-cytokine Abs followed by streptavidin-Alexa 546 (in 1× PBS with 1% BSA). The fluorescence in the microwells was imaged using a confocal microscope (Zeiss LSM 5 Pascal, Carl Zeiss, Inc., Thornwood, NY) and was analyzed with GenePix Pro 6.0 data analysis software (Molecular Devices, Downingtown, PA) to construct calibration curves of cytokine concentration *vs.* fluorescence intensity.

### Detection of TNF-α release from micorpatterned immune cells

Mouse macrophage cells (J774A) were cultured at 37°C with 5% CO$_2$ in phenol red-free Dulbecco's Modified Eagle's Medium (DMEM) supplemented with 10% fetal bovine serum (FBS). These cells were grown in suspension culture in 50 mL bioreactor tubes (Techno Plastic Products) on a rolling apparatus (Stovall). The cells were passaged two times a week by centrifuging and re-suspending in fresh culture media.

Glass pieces (~ 1 × 1 in) with microwell arrays were outfitted with PDMS microfluidic channels. Design and fabrication of the microfluidic devices have been provided in detail in our previous publications.[21, 41] Prior to cell seeding, 1 mL cell suspension was concentrated by centrifugation and was re-suspended in DMEM at ~15 million cells/mL concentration. Cell suspension was infused into the microfluidic channels and incubated for 30 min with microwells that were functionalized with TNF-α Abs as described in the previous section. Macrophages are known to attach to Fc components of Abs and became adherent inside 30 µm diameter microwells. Non-adherent cells were washed away. To induce cytokine release, macrophages were mitogenically stimulated for 3 h by 100 µg/mL PMA in DMEM. During cytokine release flow was stopped to minimize convection. After removal of PMA solution, cellular micropatterns were incubated with biotin-anti-TNF-α for 30 min followed by avidin-Alexa546 (red color). Subsequently, cells were fixed with 4% PFA for 15 min and stained with DAPI for 5 min to visualize cell nuclei. Between each step, the sample was washed with 1×PBS for 5 min to remove the previous reagent. All steps described above were performed inside a microfluidic device.

## RESULTS AND DISCUSSION

The goal of this study was to develop hydrogel microwell arrays for sensitive cytokine detection. The novelty of this paper lies in creating a bi-functional thiol/acrylate silane layer on glass, with acrylate groups promoting hydrogel attachment and thiol groups used for oriented binding of anti-cytokine Abs inside the microwells. This micropatterning strategy allowed to significantly enhance sensitivity of cytokine detection inside the microwells.

### Characterization of surface properties using ToF-SIMS and AFM

Figure 1 details our surface modification strategy involving silanization of glass substrates and micropatterning of hydrogel PEG microwells. As demonstrated in this schema, the goal was to create a mixed silane layer containing acrylate moieties for hydrogel anchoring and thiol groups for attachment of avidin/biotin-Ab constructs. Throughout this study we will be comparing sensitivity of cytokine immunoassays created on mixed silane layers to surfaces modified with mono-functional acrylated silane where avidin was physically adsorbed onto the surface.

We first wanted to verify that incubation of glass substrates with solution containing acrylate- and thiol-terminated trimethoxysilanes resulted in deposition of both types of molecules. ToF-SIMS provides an excellent means for characterizing chemical composition of surfaces and is increasingly being used for analysis of biointerfaces and micropatterned surfaces.[40, 42, 43] Cartoon in Figure 2A shows the principle of ToF-SIMS surface analysis employed here to verify coexistence of acrylate and thiol groups on glass substrates. In brief, our surfaces were analyzed by 26 keV $C_{60}^+$ ToF-SIMS running in the event-by-event bombardment-detection mode. $C_{60}$ projectiles have previously been shown by us to produce upon impact hemispherical craters 5 to 10 nm in depth.[39] Using event-by-event bombardment-detection mode we could then analyze ions co-emitted from the same impact and could determine co-existence of acrylate and thiol groups. Figure 2B shows both functional groups being present on the glass surface after silanization. Comparison of glass slides coated with acrylated silane (upper panel Figure 2B) to glass slides modified with bi-functional silane layer (lower panel Figure 2B) reveals the presence of SH derivative peaks at m/z 32 ($S^-$), 33($SH^-$), 64 ($S_2^-/SO_2^-$) and 80 ($SO_3^-$) only on the mixed silane surface. In contrast, peaks at m/z 119 ($SiCH_2+SiO_2OH^-$) and 179 ($SiCH_2+ (SiO_2)_2OH^-$) originating from acrylated silane molecules were found on glass substrates modified with both acrylated and mixed silanes.

The event-by-event technique allows to compute the fractional surface coverage of silanes. [40, 44] Briefly, two co-emitted secondary ions from an impacted/emitted nanovolume were selected to calculate individual immobilized coverage of thiol silane or acryl silane on the bifunctional surface. A fractional surface coverage of ~ 69% was obtained for the thiol silane (co-emitted ions $SH^-$ and $SO_3^-$) and ~67% for the acryl silane (co-emitted ions: $SiCH_2+SiO_2OH^-$ and $SiCH_2+ (SiO_2)_2OH^-$). This result demonstrates that the equimolar mixture of these two silanes in solution is transferred onto the surface of glass after silanization. Overall, ToF-SIMS analysis points to the assembly of both acrylate- and thiol-functionalized silanes from solution containing a mixture of the two silanes.

Beyond analysis of silane composition, SIMS was also used to verify the presence of heterobifunctional linker and avidin. Figures 2C and 2D show smaller and larger masses observed during SIMS analysis of mixed silane surfaces incubated in MAL-PEG2-NHS ester linker and avidin. Analysis of surfaces treated with linker (top spectra in Figure 2C,D) revealed presence of acrylate and thiol groups at m/z 32, 33, 119 and 179 as well as the linker at m/z 256 ($C_{11}H_{16}N_2O_5^-$) and 270 ($C_{12}H_{18}N_2O_5^-$). Surfaces incubated with avidin, showed presence of peaks associated acrylate and thiol groups as well as the linker and

avidin (bottom spectra). Negative ions at m/z 91(Phe⁻) and 107 (Tyr⁻) were assigned to amino acid residue peaks originating from avidin. In addition, substrates coated with avidin had lower intensities of glass-related masses, suggesting that protein coating was masking the underlying surface during mass spectra collection (Figure 2C). Given that the depth of projectile penetration during SIMS analysis is estimated to be 5 to 10 nm[39] the lack of glass peaks suggests dense avidin layer assembled on the substrate.

AFM was used to characterize surface topography of glass substrates modified with mono- and bi-functional silanes before and after deposition of avidin. In these experiments, physical adsorption of avidin on mono-functional silane surfaces was vs. covalent immobilization on a bi-functional (thiol/acrylate) silane layer. The latter surface was first activated with maleimide-PEG-NHS and then incubated with avidin. Figure 3(A–B) shows AFM scans before and after avidin deposition onto glass substrates modified with acrylated silane. As can be seen from these images, no appreciable changes were observed in surface topography before and after protein deposition. In contrast, AFM analysis on bi-functional silanes before and after avidin incubation reveals a significant difference in surface topography with appearance of particles ~6 nm in size. These particles correlate well to the reported size of avidin.[45] Therefore, AFM study corroborates ToF-SIMS analysis pointing to the presence of avidin on the surface and suggests that more avidin was retained on surfaces by covalent attachment.

### Fluorescence characterization of avidin adsorption inside hydrogel microwells

Commercial micro-titer plates are constantly evolving to increase the number of wells and thus improve throughput of the analyses being performed. It may be argued that arrays of microwells with dimensions similar to that of individual cells represent are best suited for high-throughput cell analysis. Therefore, there is considerable interest in microfabricating arrays of wells for cell capture and analysis.[46, 47] The approach our group has employed is to photolithographically pattern PEG hydrogel microwells on glass so that each well consists of non-fouling PEG walls and glass attachment pads (see Figure 1B).[20, 32] In this method, hydrogel attachment to glass is promoted by an acrylated silane coupling agent. However, it is almost always the case that microwells need to be further modified either with adhesive lignads to promote cell attachment or with Abs for immunosensing applications. In such a scenario, biomolecules such as avidin or ECM proteins are physically adsorbed from solution onto acrylated glass attachment pads of microwells. Protein attachment does not occur on non-fouling PEG walls of the microwells. While physical adsorption is sufficient for certain applications (e.g. cell culture) it may not suffice for immunosensing where the density and orientation of Abs are key determinants of sensor response. Therefore, our present study was focused on modifying glass substrates with a mixture of two different silane molecules to both promote gel anchoring and to enable covalent attachment of avidin as well as oriented binding of Abs inside the microwells.

It should be noted that there are other approaches for covalent attachment of proteins inside hydrogel microwells. For example, Koh and co-workers described a method whereby hydrogel structures are fabricated on amine-functionalized nanoporous substrates.[48] Hydrogel attachment on these substrates occurs based on intercalation of liquid prepolymer into the pores of the substrate prior to photo-crosslinking and does not require a silane coupling layer. While such approach is quite promising it necessitates the use of specific substrates (e.g. nanoporous alumina) whereas the method described in the present study is compatible with standard glass or plastic surfaces used in tissue culture.

To analyze protein adsorption, hydrogel microwells were fabricated on glass substrates modified with either mono-functional or bi-functional silane layers and were then incubated with fluorescently-labeled streptavidin. Figure 4(A,B) compares fluorescence in the

microwells after incubation with streptavidin-Alexa546. As seen from the images in Figure 4 (A,B), much higher fluorescence was observed in microwells modified with a bi-functional silane layer compared to mono-functional silane. This suggests that a larger number of avidin molecules were retained inside microwells by covalent binding then by physical adsorption. Quantitative analysis signal intensity (Figure 4C) shows 6 times higher fluorescence signal emanating from microwells fabricated on mixed silane layer. The data in Figure 4 are significant as they demonstrate that covalent binding to bi-functional silanes improves loading and retention of protein (streptavidin) within the microwells. It should also be noted that limited non-specific binding of avidin was observed on the hydrogel sidewalls.

## Performing cytokine immunoassays in hydrogel microwells

Building on the promising results presented in Figure 4, we wanted to determine whether higher loading of streptavidin on mixed silane surfaces would translate into more sensitive cytokine immunoassays. We chose to detect IFN-γ since production of this cytokine is commonly used to determine presence of antigen specific CD4 and CD8 T-cells in infectious diseases such as HIV and tuberculosis.[5–9] To test cytokine sensitivity, arrays of hydrogel microwells containing anti-IFN-γ Abs were exposed to IFN-γ concentrations varying from 0.5 ng/ml to 10 µg/ml. The presence of cytokine molecules inside the microwells was determined using biotinylated secondary Abs and streptavidin-Alexa 546. Figure 5 (A, B) shows representative images of microwell arrays exposed to varying concentrations of IFN-γ. As seen from a calibration plot presented in Figure 5C fluorescence intensity changed as a function of cytokine concentration with linear range extending up to 6 nM (100 ng/ml). The lower limit of IFN-γ detection for these microwells was 60 pM (1 ng/ml). This result represents a ~10 fold improvement over the limit of detection reported in our previous papers employing physical adsorption of Abs.[21, 25]

Detection of multiple cytokines from the same cell population is important in immune cell analysis and disease.[6,7] As a step towards multi-functional cell analysis, we wanted to co-deposit anti-IFN-γ and –TNF-α Abs in the same microwell arrays and to demonstrate multi-cytokine detection in microwells. In these experiments, microwells were fabricated on glass substrates containing a mixed silane and were modified with neutravidin followed biotinylated anti-IFN-γ and anti-TNF-α. Figure 6(A–D) presents a series of images from microwells challenged with TNF-α and IFN-γ dissolved in 1× PBS at 500 ng/mL (30 nM) concentration. As can be seen from these images, microwells respond to both TNF-α (red signal) and IFN-γ (green signal) suggesting that two different cytokine types may be detected in the microwell arrays. Figure 6E compares sensitivity of IFN-γ response in microwells coated with only anti-IFN-γ to microwells modified with a mixture of anti-IFN-γ and –TNF-α. This comparison points to decrease of IFN-γ signal in microwells containing a mixture of anti-IFN-γ/-TNF-α Abs. Such result is expected given that the surface density of anti-IFN-γ Abs likely 2 times lower in the case when it is co-deposited with anti-TNF-α. Despite some signal loss, the sensitivity of the IFN-γ immunoassay remains quite high. We envision immobilizing multiple Ab types in the microwells in the future to enable detection of multiple cytokines secreted by immune cells.

## Detecting TNF-α release from single macrophages in hydrogel microwells

Cytokine release from immune cells was investigated as the final step in characterization of micropatterned cytokine-sensing surfaces. Macrophages are an important leukocyte subset responsible for immune surveillance in tissue and organs. These cells robustly secrete inflammatory cytokines such as TNF-α in order to eliminate infections. Cytokine release in macrophages may be induced by stimulation with endotoxins (e.g. LPS) or mitogens. In our experiments (described schematically in Figure 7), mouse macrophages were captured in microwells created on either bi-functional or monofunctional silanes. In both cases

microwells were modified with anti-TNF prior to cell seeding. Macrophages became attached inside the microwells – this is expected given that macrophages are known to adhere to Fc domains of Abs.[49] Individual microwell dimensions of 30 µm diameter were chosen to correspond to the size of single cells. As can be seen from brightfield images in Figure 8, each microwell contained one or two macrophages. Cells captured in the microwells were stimulated with PMA (mitogen) for 3 h to induce cytokine production. Experiments were done in Petri dishes without mixing to minimize convection and to ensure that secreted TNF-α is captured in the vicinity of the cell source. Presence of secreted cytokines was determined by incubation of cellular micropatterns with biotinlyated-anti-TNF-α followed by streptavidin-Alexa546. Figure 8(B,D) show immunofluorescent staining images of macrophages captured on micropatterned glass substrates. As can be seen from these images, detection of cell-secreted TNF-α was much more sensitive in microwells containing covalently immobilized avidin-biotin-anti-TNF-α construct. It should be noted that TNF-α is not only released but is also expressed on cell surfaces. This explains cell-associated fluorescence in both types of microwells tested. Quantifying fluorescence intensity revealed that the signal in microwells with engineered avidin-Ab attachment sites was ~3 times higher than in microwells containing physically adsorbed avidin-Ab molecules (see Figure 8E) while intensity of Dapi – fluorescent dye that stains cell nucleus - was comparable in both types of microwells. The results presented in Figure 8 underscore the utility of designing attachment of recognition molecules inside microwells.

## CONCLUSIONS

The objective of this study was to design micropatterned surfaces for sensitive cytokine detection. PEG hydrogel photolithography was employed to create hydrogel microwells with non-fouling PEG walls and glass bottom. The question explored in this paper was how to engineer the glass attachment pads inside the microwells so as to increase sensitivity of cytokine immunoassays. Our solution was to move away from physical adsorption and towards covalent/oriented attachment of the sensing elements. For this purpose, glass substrates were functionalized with a binary mixture of acrylate- and thiol-terminated silanes, where acrylate groups served to anchor hydrogel microwells while the thiol groups were used to covalent link avidin in the glass attachment sites inside the microwells. A series of experiments confirmed that considerably higher density of avidin molecules was assembled in acrylate/thiol-modified microwells. This higher avidin concentration likely translated into higher Ab loading and led to a 10 fold increase in sensitivity of IFN-γ detection in microwells created on mixed silane-modified glass. Importantly, we also demonstrated ~3 times higher signal of cell-secreted TNF-α in microwells engineered for covalent avidin-Ab attachment. These more sensitive microwells will be used in the future for detection of multiple cytokines released by the immune cells. Improved sensitivity will also allow more rapid detection of cytokine release from single cells. The strategy of employing bi-functional silanes in conjunction with hydrogel micropatterning on glass has broad utility for covalent protein attachment and will have applications in cell/tissue engineering and biosensing.

## Acknowledgments

## REFERENCES

1. Tan TT, Coussens LM. Humoral immunity, inflammation and cancer. Curr Opin Immunol. 2007; 19:209–216. [PubMed: 17276050]

2. Notley CA, Ehrenstein MR. The yin and yang of regulatory T cells and inflammation in RA. Nat Rev Rheumatol. 2010; 6:572–577. [PubMed: 20808295]

3. O'Garra A, Barrat FJ, Castro AG, Vicari A, Hawrylowicz C. Strategies for use of IL-10 or its antagonists in human disease. Immun Rev. 2008; 223:114–131. [PubMed: 18613832]

4. Diel R, Loddenkemper R, Meywald-Walter K, Niemann S, Nienhaus A. Predictive value of a whole blood IFN-γ assay for the development of active tuberculosis disease after recent infection with Mycobacterium tuberculosis. Am J Respir Crit Care Med. 2008; 177:1164–1170. [PubMed: 18276940]

5. Boom H. The role of T-cell subsets in Mycobacterium tuberculosis infection. Infect Agents Dis. 1996; 5:73–81. [PubMed: 8721044]

6. Caccamo N, Guggino G, Joosten SA, Gelsomino G, Matarese A, Salerno A, et al. Multifunctional CD4 T cells correlate with active Mycobacterium tuberculosis infection. Eur J Immun. 2010; 40:2211–2220.

7. Casey R, Blumenkrantz D, Millington K, Montamat-Sicotte D, Kon OM, Wickremasinghe M, et al. Enumeration of functional T-Cell subsets by fluorescence-immunospot defines signatures of pathogen burden in tuberculosis. Plos One. 2010; 5

8. Rosenberg ES, Billingsley JM, Caliendo AM, Boswell SL, Sax PE, Kalams SA, et al. Vigorous HIV-1-specific CD4(+) T cell responses associated with control of viremia. Science. 1997; 278:1447–1450. [PubMed: 9367954]

9. Zimmerli SC, Harari A, Cellerai C, Vallelian F, Bart PA, Pantaleo G. HIV-1-specific IFN-gamma/ IL-2-secreting CD8 T cells support CD4-independent proliferation of HIV-1-specific CD8 T cells. Proc Nat Acad Sci. 2005; 102:7239–7244. [PubMed: 15872023]

10. Brando B, Barnett D, Janossy G, Mandy F, Autran B, Rothe G, et al. Cytofluorometric methods for assessing absolute numbers of cell subsets in blood. Cytometry. 2000; 42:327–346. [PubMed: 11135287]

11. Cox JH, Ferrari G, Janetzki S. Measurement of cytokine release at the single cell level using ELISPOT assay. Methods. 2006; 38:274–282. [PubMed: 16473524]

12. Karlsson AC, Martin JN, Younger SR, Bredt BM, Epling L, Ronquillo R, et al. Comparison of the ELISPOT and cytokine flow cytometry assays for the enumeration of antigen-specific T cells. J Immun Methods. 2003; 283:141–153.

13. Folch A, Toner M. Microengineering of cellular interactions. Annu Rev Biomed Eng. 2000; 2:227. [PubMed: 11701512]

14. Toner M, Irimia D. Blood-on-a-Chip. Annu Rev Biomed Eng. 2005; 7:77–103. [PubMed: 16004567]

15. Cheng XH, Irimia D, Dixon M, Sekine K, Demirci U, Zamir L, et al. A microfluidic device for practical label-free CD4+T cell counting of HIV-infected subjects. Lab Chip. 2007; 7:170–178. [PubMed: 17268618]

16. Han Q, Bradshaw EM, Nilsson B, Hafler DA, Love JC. Multidimensional analysis of the frequencies and rates of cytokine secretion from single cells by quantitative microengraving. Lab Chip. 2010; 10:1391–1400. [PubMed: 20376398]

17. Love JC, Ronan JL, Grotenbreg GM, van der Veen AG, Ploegh HL. A microengraving method for rapid selection of single cells producing antigen-specific antibodies. Nature Biotech. 2006; 24:703–707.

18. Story CM, Papa E, Hu CCA, Ronan JL, Herlihy K, Ploegh HL, et al. Profiling antibody responses by multiparametric analysis of primary B cells. Proc Nat Acad Sci. 2008; 105:17902–17907. [PubMed: 19004776]

19. Kim H, Cohen RE, Hammond PT, Irvine DJ. Live lymphocyte arrays for biosensing. Adv Mat. 2006; 16:1313–1323.

20. Revzin A, Sekine K, Sin A, Tompkins RG, Toner M. Development of a microfabricated cytometry platform for characterization and sorting of individual leukocytes. Lab Chip. 2005; 5:30–37. [PubMed: 15616737]

21. Zhu H, Stybayeva GS, Silangcruz J, Yan J, Ramanculov E, Dandekar S, et al. Detecting cytokine release from single human T-cells. Anal Chem. 2009; 81:8150–8156. [PubMed: 19739655]

22. Soen Y, Chen DS, Kraft DL, Davis MM, Brown PO. Detection and characterization of cellular immune responses using peptide-MHC microarrays. PLOS Biology. 2003; 1:429–438.

23. Bailey RC, Kwong GA, Radu CG, Witte ON, Heath JR. DNA-encoded antibody libraries: A unified platform for multiplexed cell sorting and detection of genes and proteins. J Am Chem Soc. 2007; 129:1959–1967. [PubMed: 17260987]

24. Zhu H, Macal M, George MD, Dandekar S, Revzin A. A miniature cytometry platform for capture and characterization of T-lymphocytes from human blood. Anal Chim Acta. 2008; 608:186–196. [PubMed: 18215650]

25. Zhu H, Stybayeva GS, Macal M, George MD, Dandekar S, Revzin A. A Microdevice for multiplexed detection of T-cell secreted cytokines. Lab Chip. 2008; 8:2197–2205. [PubMed: 19023487]

26. Hermanson GT. Bioconjugate Techniques. Academic Press. 1996; Vol.1

27. Blawas AS, Reichert WM. Protein patterning. Biomaterials. 1998; 19:595–609. [PubMed: 9663732]

28. Kane RS, Takayma S, Ostuni E, Ingber DE, Whitesides GM. Patterning of proteins and cells using soft lithography. Biomaterials. 1999; 20:2363–2376. [PubMed: 10614942]

29. Folch A, Toner M. Microengineering of cellular interactions. Ann Rev Biomed Eng. 2000; 2 227-+.

30. Whitesides GM, Ostuni E, Takayama S, Jiang XY, Ingber DE. Soft lithography in biology and biochemistry. Ann Rev Biomed Eng. 2001; 3:335–373. [PubMed: 11447067]

31. Revzin A, Russell RJ, Yadavalli VK, Koh W-G, Deister C, Hile DD, et al. Fabrication of poly(ehtylene glycol) hydrogel microstructures using photolithography. Langmuir. 2001; 17:5440–5447. [PubMed: 12448421]

32. Revzin A, Tompkins RG, Toner M. Surface engineering with poly(ethylene glycol) photolithography to create high-density cell arrays on glass. Langmuir. 2003; 19:9855–9862.

33. Dulcey CS, Georger JH, Krauthamer V, Stenger DA, Fare TL, Calvert JM. Deep UV photochemistry of chemisorbed monolayers-patterned coplanar molecular assemblies. Science. 1991; 252:551–554. [PubMed: 2020853]

34. Sagiv J. Organized monolayers by adsorption .1. Formation and structure of oleophobic mixed monolayers on solid-surfaces. J Am Chem Soc. 1980; 102:92–98.

35. Wasserman SR, Tao YT, Whitesides GM. Structure and reactivity of alkylsiloxane monolayers formed by reaction of alkyltrichlorosilanes on silicon substrates. Langmuir. 1989; 5:1074–1087.

36. Wayment JR, Harris JM. Controlling binding site densities on glass surfaces. Anal Chem. 2006; 78:7841–7849. [PubMed: 17105178]

37. Lee KB, Jung YH, Lee ZW, Kim S, Choi IS. Biospecific anchoring and spatially confined germination of bacterial spores in non-biofouling microwells. Biomaterials. 2007; 28:5594–5600. [PubMed: 17869337]

38. Park MA, Gibson KA, Quinones L, Schweikert EA. Coincidence counting in Time-of-Flight Mass-Spectrometry - a test for chemical microhomogeneity. Science. 1990; 248:988–990. [PubMed: 17745403]

39. Li Z, Verkhoturov SV, Locklear JE, Schweikert EA. Secondary ion mass spectrometry with C-60(+) and Au-400(4+) projectiles: Depth and nature of secondary ion emission from multilayer assemblies. Int J Mass Spec. 2008; 269:112–117.

40. Chen L-J, Shah SS, Verkhoturov SV, Revzin A, Schweikert EA. Characterization and quantification of biological micropatterns using cluster SIMS. Surf Interface Anal. 2010 published online.

41. Stybayeva G, Mudanyali O, Seo S, Silangcruz J, Macal M, Ramanculov E, et al. Lensfree holographic imaging of antibody microarrays for high-throughput detection of leukocyte numbers and function. Anal Chem. 2010; 82:3736–3744. [PubMed: 20359168]

42. Takahashi H, Emoto K, Dubey M, Castner DG, Grainger DW. Imaging surface immobilization chemistry: Correlation with cell patterning on non-adhesive hydrogel thin films. Adv Funct Mater. 2008; 18:2079–2088. [PubMed: 20700474]

43. Liu F, Dubey M, Takahashi H, Castner DG, Grainger DW. Immobilized antibody orientation analysis using secondary ion mass spectrometry and fluorescence imaging of affinity-generated patterns. Anal Chem. 2010; 82:2947–2958. [PubMed: 20230047]

44. Chen L-J, Shah SS, Silangcruz J, Eller MJ, Verkhoturov SV, Revzin A, et al. Characterization and quantification of nanoparticle-antibody conjugates on cells using C60 ToF SIMS in the event-by-event bombardment/detection dode. Int J Mass Spect. 2011 in press.

45. Kuzuya A, Numajiri K, Kimura M, Komiyama M. Single-molecule accommodation of streptavidin in nanometer-scale wells formed in DNA nanostructures. Nucl Acid Symp Ser. 2008; 52:681–682.

46. Rettig JR, Folch A. Large-scale single-cell trapping and imaging using microwell arrays. Anal Chem. 2005; 77:5628–5634. [PubMed: 16131075]

47. Charnley M, Textor M, Khademhosseini A, Lutolf MP. Integration column: microwell arrays for mammalian cell culture. Integ Biol. 2009; 1:625–634.

48. Lee HJ, Kim DN, Park S, Lee Y, Koh W-G. Micropatterning of nanoporous alumina membrane with poly(ethylene glycol) hydrogel to create cellular micropatterns on nanotopographic substrates. Acta Biomater. 2011; 7:1281–1289. [PubMed: 21056702]

49. Unkeless JC, Eisen HN. Binding of monomeric immunoglobulins to Fc receptors of mouse macrophages. J Exp Med. 1975; 142:1520–1533. [PubMed: 1194857]
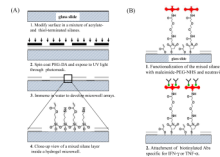
**Figure 1.**
(**A**) A process flow diagram for micorpatterning hydrogel microwells on glass. In addition to acrylate moieties used to couple hydrogel microstructures to glass, silane layer also contains thiol groups for covalent linking of proteins. (**B**) Strategy for immobilizing biomolecules inside microwells. Mixed silane layer was activated using a hetero-bifunctional cross-linker, and then incubated with avidin and biotin-antibody. Throughout this paper the sensitivity of immunoassays constructed on mixed silanes was compared to immunoassays created by physical adsorption of avidin on mono-functional acrylated silanes followed by immobilization of biotin-antibody.
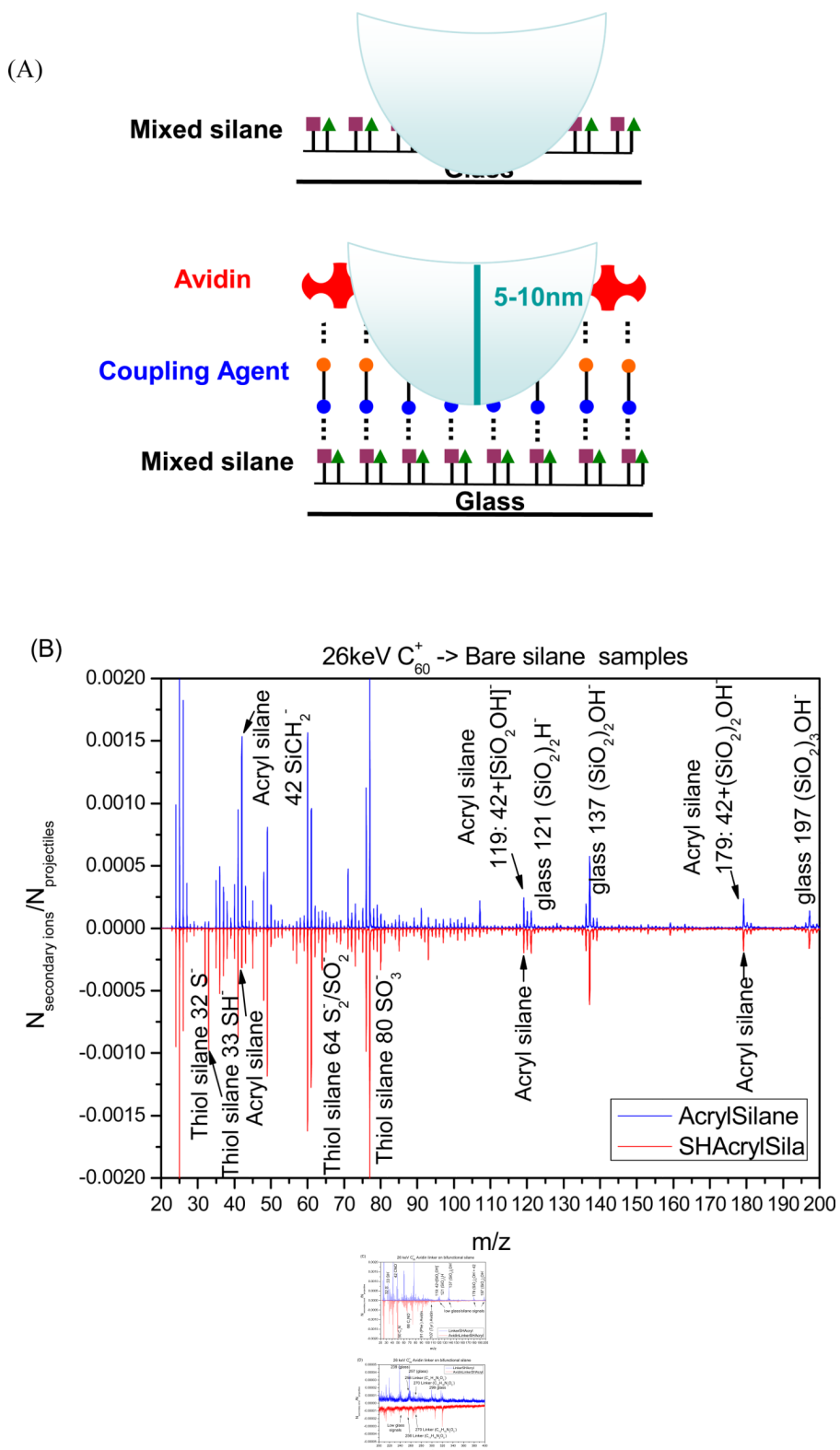
**Figure 2.**
ToF-SIMS analysis of silane modification and avidin immobilization on glass substrates.
(**A**) Schematic representation of surface bombardment with $C_{60}$ projectiles. Impact of each

projectile creates a crater 5 to 10 nm in diameter and sends ions from this volume into the SIMS instrument. Ions emitted from each impact are accounted for and provide important information about spatial co-existence of chemical species. (**B**) Comparison of negative ion mass spectra of glass substrates modified with acrylated silane (up) vs. a bifunctional thiol/ acrylated silane (bottom). This analysis reveals the presence of both acryl and thiol functional groups in the mixed silane assembled on glass. (**C–D**) The negative ion mass spectra collected from glass substrates after attachment of linker (up) and streptavidin (bottom). These spectra demonstrate presence of masses assigned to peptide bonds as well as to amino acids present in streptavidin.
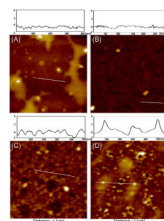
**Figure 3.**
AFM analysis of neutravidin deposition on glass substrates modified with mono- and bi-functional silanes. (**A–B**) Surface topography of glass substrates modified with acrylated silane before (A) and after (B) physical adsorption of neutravidin. (**C–D**) Surface topography of thiol/acrylate silane layer before (C) and after (D) after covalent attachment of neutravidin. Note presence of particles similar in size (6 nm) to neutravidin on glass substrates modified with mixed silane layer.
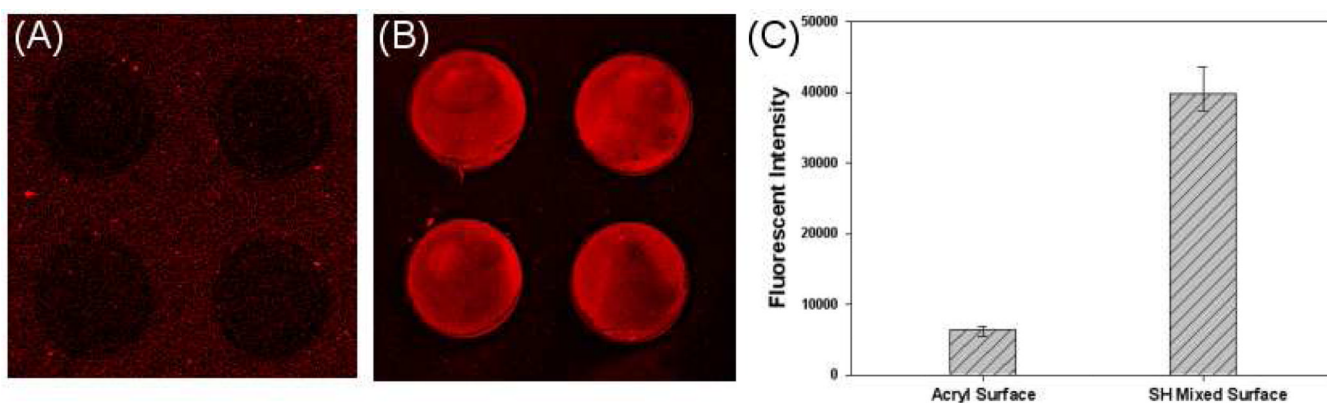
**Figure 4.**
Fluorescence microscopy analysis of streptavidin adsorption in microwells. Individual microwells were 100 µm in diameter. (**A**) Physical adsorption of streptavidin-Alexa546 in microwells containing acrylate groups in the attachment sites. Note very weak fluorescence signal observed in the microwells that is comparable to non-specific fluorescence of the hydrogel walls. (**B**) Streptavidin-Alexa546 covalent immobilized in microwells modified with thiol/acrylate silane layer. (**C**) Quantitation of fluorescence intensity showing ~6 times higher fluorescence in microwells created on a mixed silane layer.
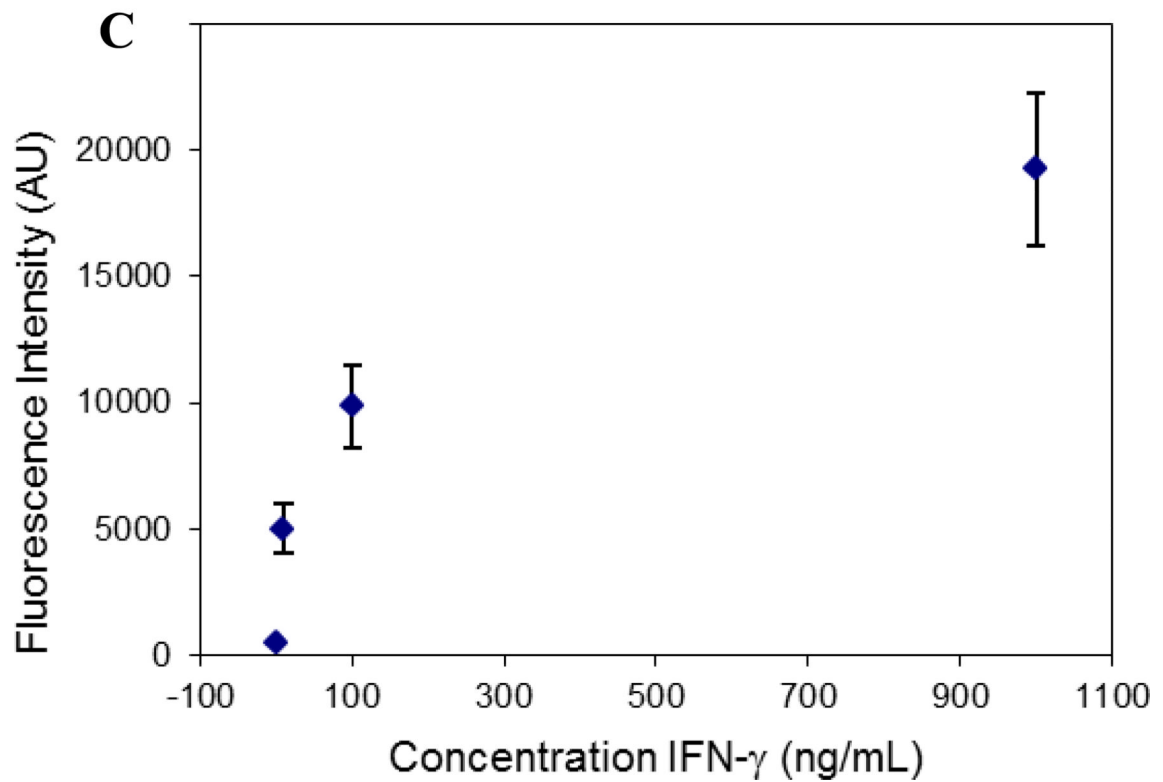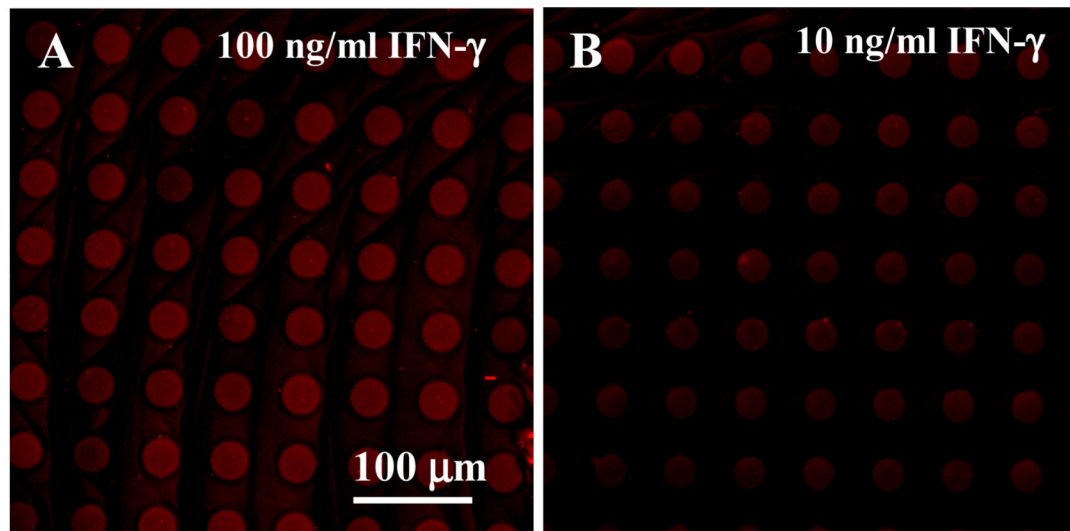
**Figure 5.**
Characterization of IFN-γ immunoassay in 30 µm microwells created on a mixed silane layer and functionalized with neutravidin and biotin anti-IFN-γ. (**A–B**) Microwell arrays were challenged with 100 ng/mL (A) and 10 ng/mL (B) of recombinant IFN-γ, then stained with anti-IFN-γ-biotin and streptavidin-Alexa546. (**C**) Calibration plot of fluorescence intensity inside the microwells vs. IFN-γ concentration. The limit of IFN-γ detection inside the microwells was 1ng/ml (60 pM).
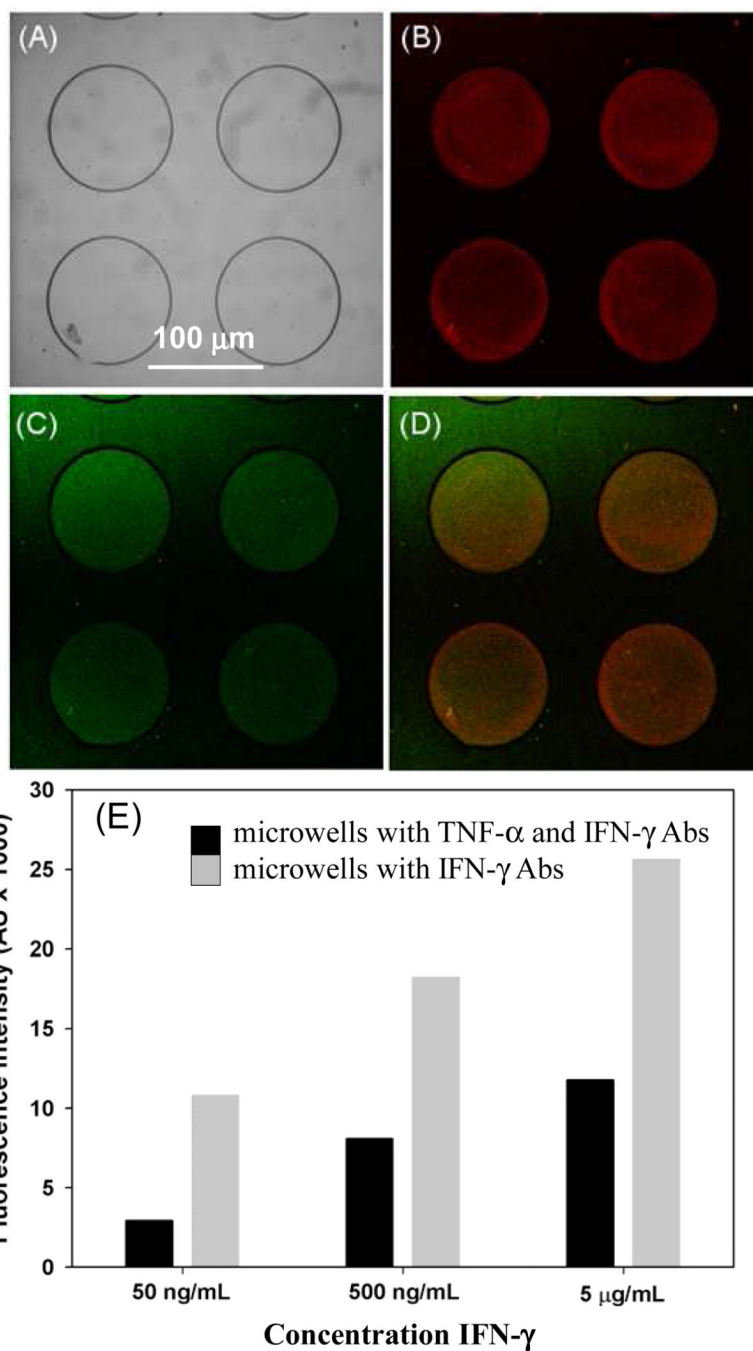
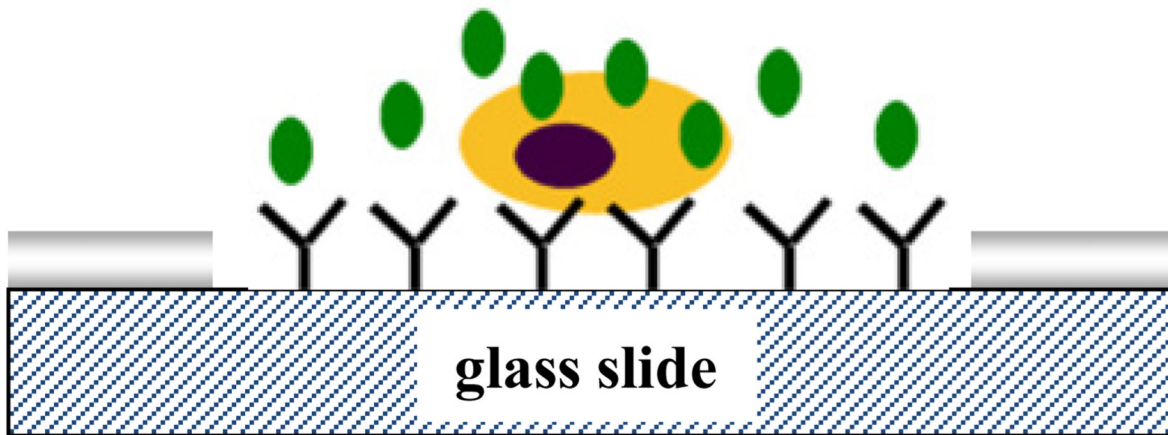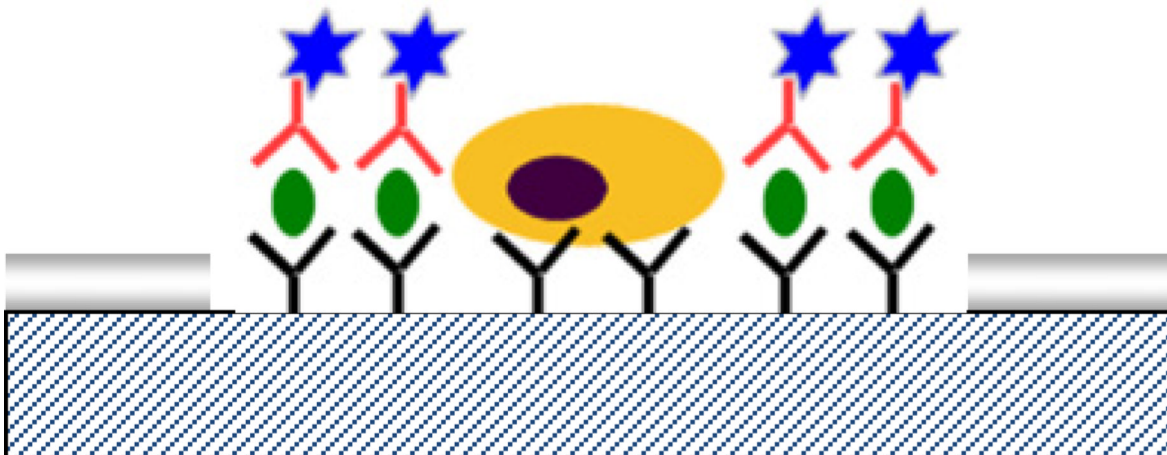**Figure 6.**
Detection of multiple cytokines inside hydrogel microwells. PEG hydrogel microwells were fabricated on a mixed silane layer, functionalized with neutravidin and then incubated with a 1:1 mixture of anti-IFN-γ and anti-TNF-α Abs. (**A**) Brightfield image of hydrogel microwells. (**B–D**) These microwells were simultaneously challenged with 500 ng/mL IFN-γ and TNF-α, subsequently microwells were incubated in a mixture of anti-IFN-γ-PE and anti-TNF-FITC. Images show both red and green fluorescence inside the microwells demonstrating that the two cytokines could be detected simultaneously. (**E**) Characterizing sensitivity of cytokine immunoassay as a function of Ab immobilization. Responses to 500

ng/mL (30 nM) IFN-γ were compared for microwells modified with anti-IFN-γ as well as microwells containing anti-IFN-γ/anti-TNF-α combination.

**glass slide**

1. Single macrophages captured in microwells containing anti-TNF-α.

2. Activation of macrophages results in secretion of TNF-α and capture of this cytokine in microwells.

**Figure 7.**
Schematic describing cytokine release studies. Step 1: Macrophages were captured inside microwells pre-coated with anti-TNF-α Abs. Cells were mitogenically activated to induce cytokine production. Step 2: Binding of secreted TNF-α inside the microwells was determined by sandwich immunoassay. Fluorescence cytokine signal was co-localized with specific cytokine-producing macrophages.
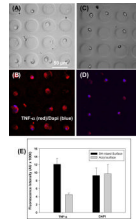
**Figure 8.**
Detection of TNF-α release from individual macrophages. PEG hydrogel microwells (30 µm diameter) were precoated with anti-TNF-α Abs and incubated with cells. (**A–D**) Imaging of macrophages in hydrogel microwells. Brightfield images of cells captured in microwells constructed on mixed silane (A) and mono-functional silane (C). Immunofluorescent staining for TNF-α production in activated macrophages (B and D). Cells were mitogenically stimulated for 3 h and then stained with anti-TNF-α-biotin followed by streptavidin-Alexa546. Cell nuclei were stained with Dapi (blue color). (**E**) Characterization of TNF-α fluorescence in microwells created on bi-functional or mono-functional silanes. Microwells with covalently immobilized avidin-biotin-Ab construct had 3 fold higher fluorescence signal compared to sensing microwells created on monfunctional silanes. Dapi intensity was the same for cells captured in both types of microwells. `The signal represents an average fluorescence in 20 microwells.